Static and Dynamic Behavior of Unbonded Elastomeric Bridge Bearings

Kemal Arman Domanic

Abstract A positive connection between superstructure and substructure in vertical or horizontal directions cannot be achieved by use of unbonded elastomeric bearings. The horizontal connection of unbonded bearings to the structure is furnished thru friction at contact surfaces while gravitational forces are utilized to maintain contact in vertical direction. An approximate horizontal friction coefficient of 0.20 is typically used at contact surfaces in seismic design based on practice in Turkey. The aim of this study is to identify the static and dynamic characteristics of these unbonded bearings thru an experimental program. In this scope, about a half scale bridge, having a 12 m span length with a 3.5 meter wide concrete deck on three steel I-beams, was constructed on a shake table. Static response of bearings was measured using a combined compression-shear bearing test machine. The experimental results indicated that bonded and unbonded bearings exhibited a similar seismic performance when excited to the same earthquake record. Use of a horizontal friction coefficient of 0.20 in seismic analysis can yield to underestimation of substructure design forces and significant overestimation of seismic displacement demands. A comprehensive parametric study was performed to identify dynamic response of similar simple-span bridges in terms of deck displacements and bearing shear forces.

1 Introduction

Unbonded elastomeric bearings are usually placed on the cap beams or the piers by having no means of positive connection besides friction. Post-earthquake investigations [1, 2, 3 and 4] suggested that significant bridge damage could occur in such cases. Compressive stresses in bearings can significantly decrease during seismic activity, yielding a reduction in lateral contact [5, and 6]. Unbonded bearings can even walk out of its supports [7], due to only thermal movements.

In Turkey, a common value of 0.20 is frequently used for horizontal friction coefficient at contact surfaces although its use is suggested only under service loads per specifications [8 and 9]. In this scope, bearing shear tests, bridge shake table tests and parametric studies were conducted to identify the realistic dynamic behavior of unbonded elastomeric bearings.

2 Combined Compression & Shear Response Tests

Unbonded and bonded bearings are tested under combined compression and shear to determine their performances in terms of effective stiffness and damping. Calculated values are presented in Figure 2. Unbonded bearings of Type 2 & 3 exhibited similar shear stiffness and damping.

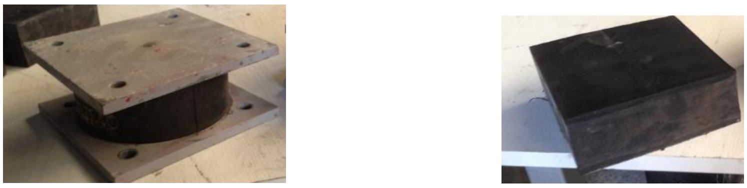

(a) Bonded bearings (b) Unbonded bearings

Fig. 1. Bonded and unbonded elastomeric bearings used in the test setup

Table 1. Bearing geometric properties

Bearing Type	Shape	Dimensions (mm)	# of Rubber Layers	Thick. of an Int. Rubber Layer (mm)	Thick. of an Ext. Rubber Layer (mm)	Thick. of Steel Shim Plates (mm)
Type-1	Circular	D_b=150	5	10	N/A	2
Type-2	Square	150x150	4	8	4	2
Type-3	Square	150x150	4	8	4	(Fiber)

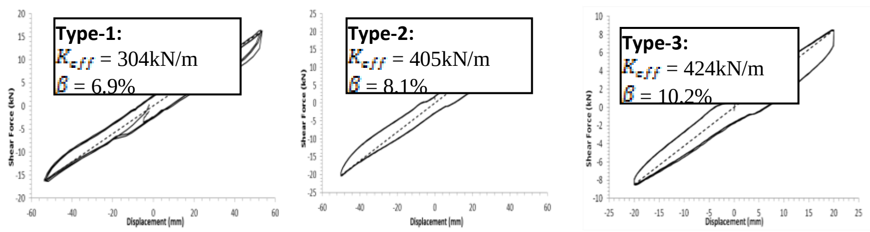

Fig. 2. Hysteresis loop obtained from combined compression-shear tests

3 Bearing Lateral Contact Force Tests

Static shear tests were performed on Type-2 bearings to estimate the lateral contact force between steel and rubber. A maximum of 100 mm lateral displacement was applied.

Prior to testing, steel plates with different surface characteristics are used to evaluate the sensitivity on measured contact forces (Figure 3). Steel surface type did not have a significant effect on behavior and obtained response was nearly identical with the clamped compression-shear test results (Section 2); i.e. zero to negligible slipping occurred at highest loading rate of 500 mm/min.

Shear force (total force of two bearings) vs. lateral bearing displacement graphs are presented in Figure 4. Loading rate had a significant effect on the lateral contact force between bearings and steel plates. At higher load rates, the ratio of lateral contact force to vertical force is about two times the ones determined for slow loading rates. The bearings have tendencies to slip at slow load rates and to roll at higher load rates.

As expected, at low level vertical forces, the ratio of lateral force to vertical force is much higher than the ones measured at high level vertical forces.

(a) Slightly rusted stainless (b) Moderately sanded and galvanized (c) Raw (d) Galvanized

Fig. 3. Steel surface finishes used in cyclic friction tests (load rate = 500 mm/min)

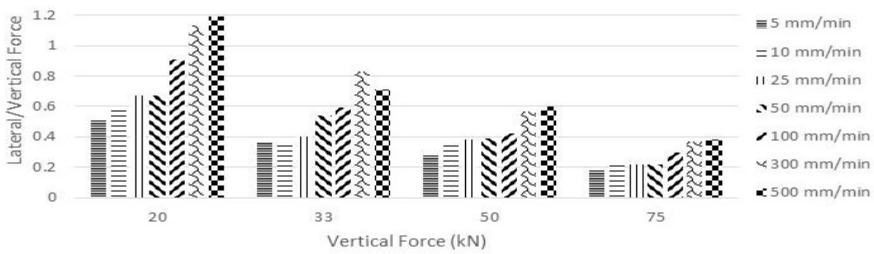

Fig. 4. Ratio of lateral to vertical forces at different load rates

4 Descriptions of the Bridge Setup and Instrumentation

A single span bridge having 12m deck length and 3.5m deck width was constructed at the METU Civil Engineering Department K2 Laboratory.

Superstructure consisted of a 150 mm thick concrete slab on three IPE400 steel girders spaced 1m apart, connected with K-shaped cross-frames constructed with single angle steel profiles at every 1.3m along its length (Figure 5).

Concrete had achieved an average compressive strength of 25MPa at 28 days. Structural steel had minimum yield strength of 275MPa. All mild reinforcements were manufactured from S420 grade steel.

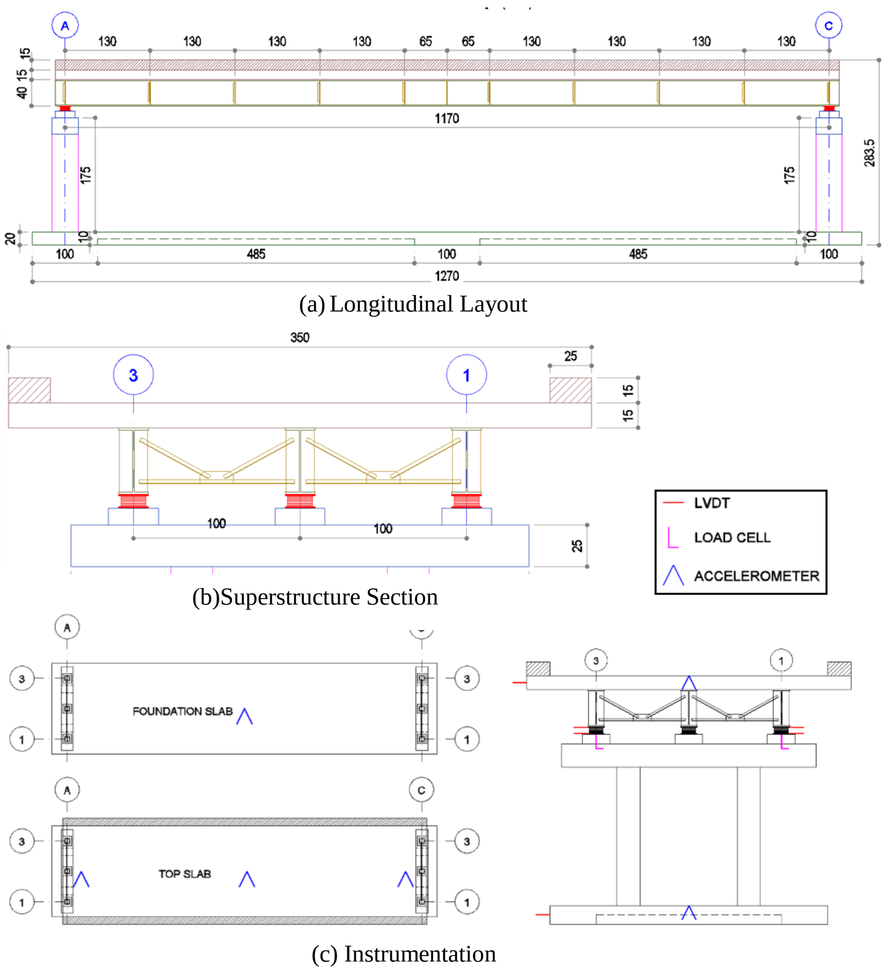

Fig. 5. Details and instrumentation of the bridge setup with bearing and pier axes labels

The same bridge setup was tested with bonded and unbonded types of bearings. The layout of bearings presented in Table 2. Bridge test monitoring system including load cells, accelerometers and LVDT's are depicted in Figure 5.

Table 2. Bearings used at test setups

Bridge Setup	Used Bearings	Bearing Connection
Bonded	6 x Type-1	M12 Bolts
Unbonded	2 x Type-2 (Middle) and 4 x Type-3 (Sides)	N/A

5 Static Bridge Load Tests

A setup was prepared to push the bridge longitudinally to estimate the ratio of lateral contact forces to vertical force under low level loading rates (Figure 6).

Load vs. displacement curves obtained from bridge test diverged from bearing tests at a force value of 41.9kN (Figure 7 and Table 3, point 1), indicating the point of slipping. The coefficient of friction value where slipping starts was calculated as at most 0.20. When longitudinal force reached up to 57.6kN (point 2), full slipping was observed yielding a static friction coefficient of 0.29. After loading was stopped (point 3), slipping continued until the load decreased to 40.3kN (point 4), suggesting to a dynamic coefficient of friction of at most 0.20.

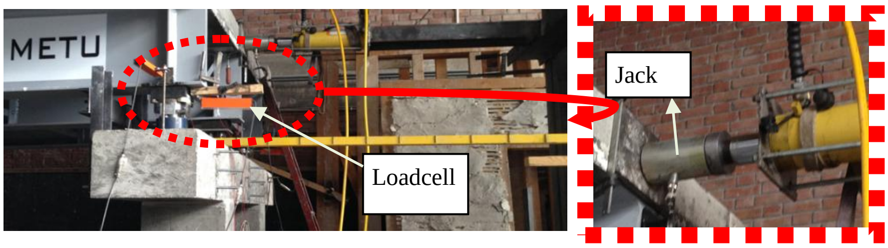

Fig. 6. Test setup for static loading

Table 3. Measured force and displacement during static loading test

Point	F (kN)	Δ (mm)
1 (Initial slip)	41.9	15.4
2 (Full slipping)	57.6	33.3
3 (Loading stopped)	57.9	37.1
4 (Unloading)	40.3	40.9
5 (End)	0.0	23.4

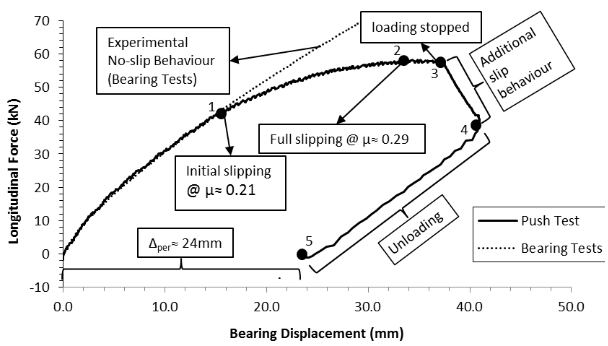

Fig. 7. Results obtained from static loading test

6 Seismic Shake Table Tests and Comparison with FEA Results

The selected motions represent scaled responses of actual earthquake records (Table 4).

Table 4. Summary of Seismic Motions

EQ	Eartquake	Mw	Station	Local Site Soil Type	Scale Factor	Scaled PGA
M1	Kocaeli 1999	7.4	Sakarya	C	0.397	0.213
M2	Kocaeli 1999	7.4	Sakarya	C	0.200	0.107
M3	Kocaeli 1999	7.4	Goynuk	D	1.000	0.135
M4	Duzce 1999	7.2	Duzce	D	0.370	0.124
M5	Duzce 1999	7.2	Duzce	D	0.200	0.067

Maximum responses of bonded and unbonded bearing system were obtained at tests of M4 ground motion record. The bearings did not have any absolute uplift.

No permanent lateral displacements of bearings or deck were observed. No slip was observed even for unbonded case. Maximum relative velocity of top of bearings with respect to bottom was 236 mm/s for bonded case where the same value was observed to be 172 mm/s for unbonded case.

Comparison of experimental data and FEA results of the bonded and unbonded setups are presented in Figure 8. Bearing displacement histories were in good agreement with test results. Larger compressive bearing forces had been observed in shake table tests. FEA results followed up almost similar patterns of ups and downs recorded during the tests.

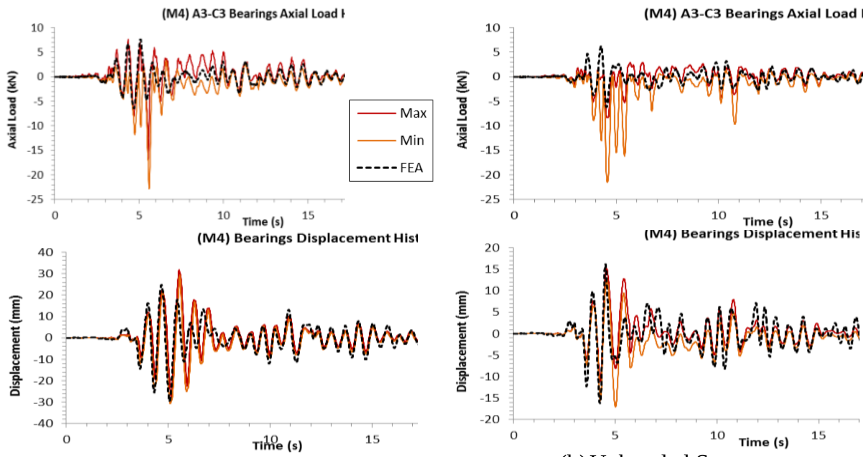

(c) Bonded Setup (b) Unbonded Setup

Fig. 8. Comparison of experimental data and FEA results

7 Parametric Studies

A comprehensive parametric study consisting of approximately 800 nonlinear time-history analyses using spectrum compatible ground motion records (S1 to S3) conducted to investigate the sensitivity of the structure to various friction coefficient, seismic acceleration, skew angle and bearing shear stiffness.

8.1 Effect of Friction Coefficient and Acceleration Coefficient

Deck displacements increased rapidly when coefficient of friction is smaller than a particular value. The critical particular value was between 0.15-0.30, depending on the seismic acceleration.

Normalized resultant deck displacements with respect to the response obtained using linear bearing elements for the same system without any friction interface are plotted on Figure 10. For low seismic hazard (A= 0.10), no significant amplification of deck displacements was observed provided that friction coefficient was greater than 0.20. For higher seismic loadings, deck displacements were stable in the friction coefficient range of 0.30-0.60, increasing outside the range. Most likely in this range, the bearings do not reach the shear force to have sliding effect.

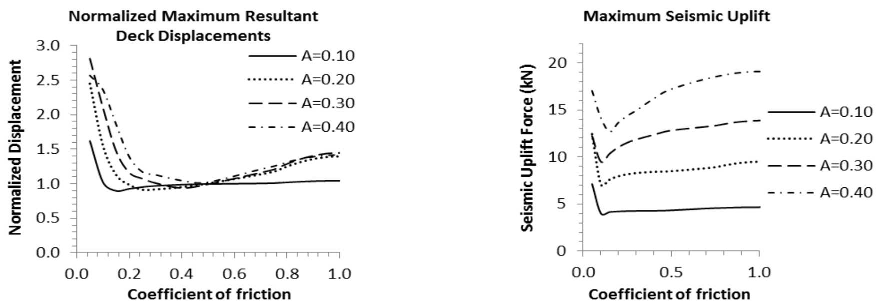

Fig. 9. Maximum resultant and normalized deck displacements as a function of friction coefficient and maximum seismic uplift forces

A decrease in seismic uplift force occurred where friction coefficient is approximately 0.10, magnitude of uplift was not observed to be highly dependent to friction coefficient values greater than 0.30 as expected.

At friction coefficients between 0.20-0.50, maximum deck displacement and coefficient of acceleration seemed to be in approximately linear direct proportion indicating that non-linear response was not observed such as slip response.

At friction coefficient range 0.30-0.50, resultant normalized deck displacement was nearly constant and independent of the friction coefficient. An approximately linear relation also existed between seismic uplift force and acceleration coefficient for μ=0.15-0.75.

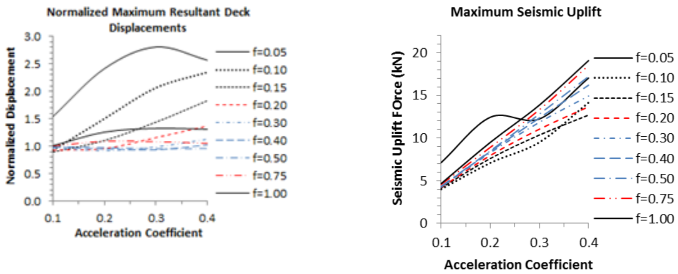

Fig. 10. Normalized maximum resultant relative deck displacements and seismic uplift forces as a function of acceleration coefficient

8.3 Effect of Skew and Fundamental Frequency

Results indicated that skew angle of the bridge did not have a significant effect on maximum and permanent deck displacements as well as with bearing axial forces. This outcome was expected indeed, as fundamental modes in lateral and longitudinal directions were uncoupled and fundamental frequencies were nearly the same regardless of skew angle of the bridge.

Results indicated that normalized displacements were affected by fundamental frequency to an extent and an irregular relation exists between two. Dependence was more significant for moderate to high seismic loading (A=0.30-0.40). Dependence of maximum seismic uplift forces in bearings to fundamental frequency of the system was less pronounced. An approximately linear relation seemed to exist between the two.

8.5 Extended FEA and Trendline Construction

Results of the parametric study pointed out to a possibility of a simple and reasonably approximate correlation between maximum resultant deck displacements normalized by the responses of corresponding bonded system and acceleration coefficient when friction of coefficient is over 0.20.

Additional FEA of 16 bridge setups using response spectrum compatible earthquake records S4 to S9 were performed to calculate maximum deck displacements normalized by the responses from linear counterpart of each setup.

Chosen parameters are summarized in Table 4. Graph of calculated normalized resultant deck displacement vs. acceleration coefficient is presented in Figure 11.

Table 4. Properties of analyzed FEA configurations

Model #	Record #	A	μ	t (s)	freq. (Hz)	Skew (°)	h/w
1	S4	0.1	0.40	0.836	1.196	50	0.25
2	S5	0.1	1.00	0.836	1.196	10	1.00
3	S6	0.1	0.30	1.648	0.607	60	0.75
4	S4	0.2	0.75	0.603	1.658	50	0.25
5	S5	0.2	0.25	0.442	2.262	30	0.50
6	S6	0.2	0.50	1.171	0.854	0	0.50
7	S4	0.3	0.75	1.648	0.607	10	0.25
8	S5	0.3	0.30	1.171	0.854	20	2.00
9	S6	0.3	0.50	1.648	0.607	0	0.75
10	S4	0.4	0.40	0.603	1.658	40	1.50
11	S5	0.4	0.25	0.836	1.196	60	0.75
12	S6	0.4	1.00	1.171	0.854	30	0.25
13	S7+S8+S9	0.1	0.40	1.648	0.607	0	0.50
14	S7+S8+S9	0.2	0.50	0.442	2.262	40	0.25
15	S7+S8+S9	0.3	0.30	0.603	1.658	20	0.50
16	S7+S8+S9	0.4	0.75	0.442	2.262	0	0.25

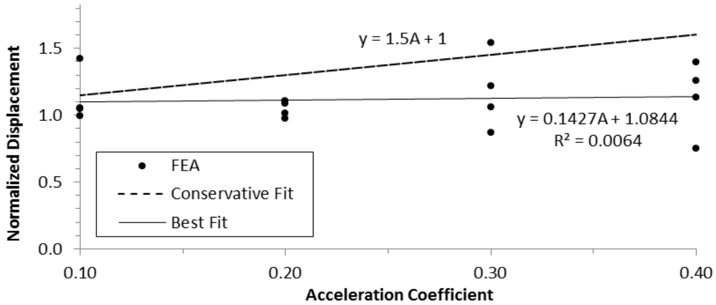

Fig. 11. Normalized maximum deck displacements obtained from FEA of additional cases as a function of acceleration coefficient

An approximate estimation of deck displacements could be obtained as:

- Calculate the resultant bearing displacements using linear bearing elements (simulating bonded bearings).
- Multiply the calculated displacement by a correction factor of:
  C=1.0+1.5A; where A is the acceleration coefficient

Forces transferred to substructure may also be calculated as the maximum of:

- Bonded response at the calculated unbonded displacement response
- $1.10D_L$, where D_L is the dead load action on the bearing

9 Conclusions

Static friction coefficient between various steel surface finishes and elastomeric bearings were measured to be between 0.29-0.40 under very low loading rates.

Results indicated that coefficient of friction is highly dependent on loading rate. For moderate to high loading rates (greater than 300 mm/min), bearing slipping was not observed for unbonded case. Results of shake table tests also indicated that unbonded bearings were unlikely to slip under seismic loading (e.g. rates higher than 3000mm/min).

A friction coefficient of 0.20 is frequently considered for seismic design in Turkey. Use of such values can be unconservatively low for seismic analysis to determine substructure forces while significantly overestimating seismic displacement demands, and may not properly represent the interaction of bearings and the structure during seismic loading. Such values should not be used in seismic design unless indicated otherwise by validated test data.

A simple formulation defining a conservative trendline for unbonded deck displacements as a function of acceleration coefficients was presented. A simplified procedure is also included to estimate shear forces transferred from unbonded bearings to substructure.

Acknowledgments The authors would like to thank to TÜBİTAK for technical and financial support and to Nefize Shaban for her invaluable contribution to the study presented herein. They also would like to extend their appreciation to General Directorate of Highways (KGM).

References

1. ASCE-TCLEE (1999), "Lifelines Performance, Kocaeli, Turkey Earthquake, August 17, 1999", ASCE, Technical Council on Lifeline Earthquake Engineering
2. Pamuk A., Kalkan E., Ling H.I. (2005), "Structural and geotechnical impacts of surface rupture on highway structures during recent earthquakes in Turkey", Soil Dynamics and Earthquake Engineering, Vol.25, 581-589
3. Papazoglu A. J. and Elnashai A. S. (1996), "Analytical and Field Evidence of The Damaging Effect of Vertical Earthquake Ground Motion", Earthquake Engineering & Structural Dynamics, Vol.25, No.10, 1109-1137
4. Yen W. P., Ghasemi H. and Cooper J. D. (2001), "Lessons Learned from Bridge Performance of the 1999 Turkish & Taiwan Earthquakes", 33rd Joint Meeting of the UJNR Panel on Wind and Seismic Effects, Tsukaba, Japan
5. Domaniç K. A. (2008), "Effects Of Vertical Excitation On Seismic Performance Of Highway Bridges And Hold-Down Device Requirements", MS Thesis, Middle East Technical University
6. Mitoulis S. (2014), "Uplift of Elastomeric Bearings in Isolated Bridges Subjected to Longitudinal Seismic Excitations", Structure and Infrastructure Engineering
7. Yura J., Kumar A., Yakut A., et al (2001), "NCHRP Report 449 - Elastomeric Bridge Bearings: Recommended Test Methods", The University of Austin, Texas
8. AASHTO (2002), "Standard Specifications for Highway Bridges, 17th Edition", AASHTO
9. AASHTO (2012), "LRFD Bridge Design Specifications", AASHTO